Formulation of a Consistent Multi-Species Canopy Description for Hydrodynamic Models Embedded in Large-Scale Land-Surface Representations of Mixed-Forests

G. Bohrer[1], J. E. C. Missik[1]

[1]Ohio State University, Department of Civil, Environmental & Geodetic Engineering.

Corresponding author: Gil Bohrer (bohrer.17@osu.edu)

Key Points:

- New generation of plant-hydrodynamic land surface models require resolution representative of characteristic individual trees.
- Tree-level flux representation diverges from the common area-based representation, especially in mixed plots of multiple species or types.
- We provide a formulation using common crown characteristics for consistent scaling of leaf- and tree-level fluxes to area-based plot level.

Abstract

The plant hydrodynamic approach represents a recent advancement to land surface modeling, in which stomatal conductance responds to water availability in the xylem rather than in the soil. To provide a realistic representation of tree hydrodynamics, hydrodynamic models must resolve processes at the level of a single modelled tree, and then scale the resulting fluxes to the canopy and land surface. While this tree-to-canopy scaling is trivial in a homogeneous canopy, mixed-species canopies require careful representation of the species properties and a scaling approach that results in a realistic description of both the canopy and individual-tree hydrodynamics, as well as leaf-level fluxes from the canopy and their forcing. Here, we outline advantages and pitfalls of three commonly used approaches for representing mixed-species forests in land surface models, and present a new framework for scaling vegetation characteristics and fluxes in mixed-species forests. The new formulation scales fluxes from the tree- to canopy-level in an energy- and mass-conservative way and allows for a consistent multi-species canopy description for hydrodynamic models.

1 Introduction – why tree-level fluxes are inconsistent with current surface flux representation

Representation of canopy and tree function in earth system models (ESMs) has gone through rapid advancements in the last decade. The classical big-leaf representation of the forest canopy [*Farquhar et al.*, 1989; *Sellers et al.*, 1992] in land surface models (LSMs) is being expanded and replaced by more complex canopy representations. The complexity of canopy representation in LSMs is advancing in multiple dimensions. One dimension of canopy complexity is functional diversity. Models vary in the number and exact definitions of functional types they can represent. Nonetheless, almost every modern LSM can handle the representation of structural/functional diversity of the ecosystem through sets of pre-calibrated parameters describing land-cover classes and plant functional types (PFTs), equivalent to or more detailed than the International Geosphere–Biosphere Programme (IGBP) land-cover classification system [*Loveland and Belward*, 1997]. More complex canopy models can represent age/size stages within functional types [see review by *Fisher et al.*, 2018]. A second dimension of complexity includes the spatial heterogeneity of the canopy, which can be represented by multiple "plots" within a model grid-cell with different canopy height and leaf area characteristics. Finally, a third dimension of complexity is the vertical structure of the canopy. Major advances have been made in the representation of structural complexity of canopies along the vertical dimension, by including vertically detailed representations of leaf density with between two canopy-leaf layers [representing light and shade leaves, as in the CLM model, *Dai et al.*, 2004] to *n* canopy-leaf layers [for example in an advanced version of CLM, *Bonan et al.*, 2021; *Bonan et al.*, 2018]. Advancements in remote sensing and ground-based optical techniques using high resolution lidar and hyperspectral images make it possible to interpret tree-level information from remote sensing data. These data can be used for resolving horizontal heterogeneity and tree-crown characteristics [e.g., *Detto et al.*, 2013; *Garrity et al.*, 2012; *Simard et al.*, 2011], functional/species/trait identity and diversity [e.g., *Schweiger et al.*, 2018; *Serbin et al.*, 2014; *Sothe et al.*, 2019], and vertical canopy structure [e.g., *Atkins et al.*, 2018; *Lefsky et al.*, 2002; *Yu et al.*, 2017].

The plant hydrodynamic approach represents an advancement to land surface modeling, and LSMs and ESMs have recently started including a hydrodynamic version [*Christoffersen et al.*, 2016; *Kennedy et al.*, 2019; *Lawrence et al.*, 2019; *Li et al.*, 2021; *Xu et al.*, 2016]. Under the hydrodynamic approach, stomata respond to water availability (represented as water content or water potential) in the xylem, rather than directly responding to soil water availability. The result is a model that includes the stem and/or stem xylem as potential spaces for water storage, and as conduits for water. The stem and xylem characteristic dimensions (area, diameter, volume, etc.) are needed by such models for determining the flow and storage of water in the stem/xylem.

Current, non-hydrodynamic LSMs represent vegetation at the site-level, corresponding to the discretized spatial pixel of the atmospheric column model, and/or at the plot-level, corresponding to the horizontally averaged representation of the vegetation of a particular land cover or PFT. Different models use different terminology to the describe the smallest resolved spatial unit (e.g., site, pixel, grid-cell), and the PFT-specific sub-grid scale unit (e.g., plot, tile, patch). Throughout this manuscript we will use 'site' for a single resolved land unit and 'plot' for the PFT-specific sub-grid-scale unit within a site. Consistent with the per ground area resolution of fluxes and the atmospheric column, the surface and canopy characteristic dimensions are either normalized per ground area (e.g., leaf area index, LAI) or provided in units of length (e.g., rooting depth, roughness length, canopy height). Hydrodynamic models require a revised approach to discretization of model canopies to the tree level, a distinctly different scale than the site or plot levels.

As demonstrated by *Bohrer et al.* [2005], tree hydrodynamics are strongly dependent on the allometry of tree height, stem diameter, xylem area, and taper function (i.e., how the stem diameter/area change with height). Furthermore, the stem xylem acts as a combined water storage space and a central conduit to water transport from the soil, which serves the entire crown. Therefore, for the purpose of resolving realistic tree hydrodynamics, it is imperative to preserve the relationships between the total leaf area supported by a single crown, the height of the crown, the xylem area and volume, and the vertical profiles of xylem area and leaf area throughout the crown, which requires a set of intrinsic characteristic length scales describing an individual tree (Fig. 1). For an individual tree, a crown with a large ground-projection area is supported by a stem with a conductive active xylem cross-sectional area. The stem and xylem cross-section areas are much smaller than the crown projection area. Like the crown, the roots explore a certain volume with a horizontal projection area that is much larger than the stem. A challenge for all hydrodynamic approaches is that diameter, height, area, and volume do not scale linearly [see example for allometric scaling functions relating height, crown and DBH, *Garrity et al.*, 2012]. Furthermore, the equations that describe the hydraulic relationships between water content and conductivity to water flow are strongly non-linear and depend both on the volume and the conductive area of a stem element. For example, the combined crown area of five small trees with stems with a diameter at breast height, DBH (the common measure of stem size) of 10 [cm DBH], and a corresponding basal cross-section area of 314.16 [cm^2] could be much larger (or could be smaller) than the crown area of a single tree with stem diameter of 50 cm (corresponding with basal area of 7853.98 [cm^2]), or a stem cross-section area of $5 \times 314.16 = 1570.80$ [cm^2] (corresponding with a DBH of 22.36). Furthermore, for a particular tree species, the characteristic height of a tree with a DBH of 10 [cm] is different than that of a 50 [cm DBH]- and 22.36 [cm DBH]-trees. There are infinite permutations of trees with different characteristic sizes but the same leaf area index (m^2 leaves per m^2 ground area). Because both the conductive area (for transpiration and sap flow) and the hydrostatic water potential in the xylem (a function

of volumetric water content) are important to the dynamics of moving water through the conductive system of the tree, and because crown area, leaf area, and height are important to the strength of evaporative demands, adding x% more xylem volume by growing x% taller and maintaining a constant stem and crown cross-sectional areas will have very different consequences than adding the same x% more crown and stem-xylem areas while maintaining constant height.

A trivial, intuitive scaling from the tree to the plot level involves multiplying the tree-level (total per tree) flows by the stand density (number of trees per unit plot area). However, when scaling up from the tree to the canopy scale, there is no guarantee that the tree crowns continuously and uniformly cover the whole plot area. In sparse forests, the average distance between trees may be larger than the crown diameter, whereas in dense forests, individual tree crowns may overlap and the mean distance between trees may be smaller than the crown diameter. This leads to a discrepancy between the meaning of LAI in hydrodynamic models (at the tree scale) and general land surface models (at the plot scale). Hydrodynamic models must explicitly represent all the transpiration from the entire crown, as all transpiration from a crown flows through a single stem. That means that evaporative demands and transpiration rates are considered per the area relevant to tree, i.e., the ground area projected under the crown, rather than the ground area of the whole plot (Fig. 1). As the total area under the crowns (crown area × number of trees in the site) does not necessarily equal the plot area, special considerations must be given to scaling LAI and tree-level fluxes, which despite having the same physical units, in a hydrodynamic tree-level model are provided per ground area under the crown, whereas the land surface model requires fluxes per ground area in the plot.

The overall plot-level leaf area index (LAI_p) is currently the most observed and commonly used site-level characteristic of vegetation canopies. Worldwide observations of LAI_p exist from remote sensing products and plot-level optical measurements. LAI_p represents the average leaf area per ground area for an entire plot [m^2 leaf/m^2 ground]. In a mixed forest it includes leaves of multiple species (sp), such that

$$LAI_p = \sum_{sp=1}^{N_{sp}} LAI_p^{(sp)} \quad (1)$$

where $LAI_p^{(sp)}$[m^2 leaf of (sp) /m^2 ground] is the species-specific leaf area index per unit ground area in the plot and N_{sp} is the number of species in the plot. $LAI_p^{(sp)}$ is typically measured using leaf-litter traps and could also be characterized by remote sensing using high-resolution multi-spectral images combined with spectral characterization of different tree types [*Ju and Bohrer*, 2022; *Sothe et al.*, 2019; *Yu et al.*, 2017]. Currently, $LAI_p^{(sp)}$is available in some plots but is not a very commonly reported property of forest plots. Splitting $LAI_p^{(sp)}$ to further distinguish among size categories is harder and not commonly done. Nonetheless, any modeling approach that resolves two different species requires $LAI_p^{(sp)}$, and therefore current modeling efforts already must make some assumptions about $LAI_p^{(sp)}$ values at any given plot.

A different approach to view species-specific leaf area index is the ground accumulated leaf area per unit ground-projection under the tree crowns of each species, $LAI_c^{(sp)}$ [m^2 leaf of (sp) / m^2 ground under (sp) crowns]. Importantly, this is the leaf area that is supported by individual crowns, and therefore it is $LAI_c^{(sp)}$ that characterizes the virtual hydrodynamic model

tree crowns for each type. While it is possible to measure $LAI_c^{(sp)}$ in many individual crowns using ground-based optical methods with a narrow upward cone, or by combining lidar and multispectral images, it is rarely done or reported as plot characteristic. Nonetheless, we can use the relationship between $LAI_c^{(sp)}$ and $LAI_p^{(sp)}$ to determine a plot-characteristic crown-level $LAI_c^{(sp)}$:

$$LAI_p^{(sp)} = LAI_c^{(sp)} \times A_c^{(sp)} \times 0.0001 SD^{(sp)} \quad (2)$$

where $A_c^{(sp)}$ [m^2] is the characteristic ground-projection area of crowns of (*sp*) (Fig. 1), $SD^{(sp)}$ [ha^{-1}] is the species-specific stand density (i.e. the number of tree crowns of (*sp*) per unit plot area in hectares), and 0.0001 is the conversion factor from hectare^{-1} to m^{-2}.

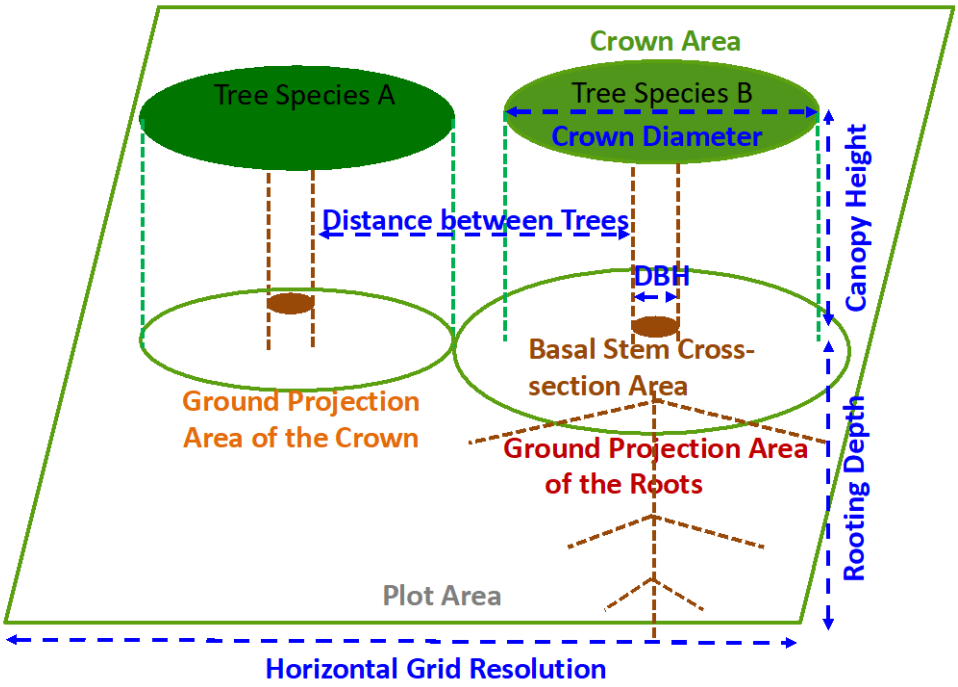

Figure 1. Schematic illustration of the characteristic length scales and areas for species-specific crowns and whole-plot descriptions of canopies.

The difference between the tree-level description of the hydrodynamic canopy and the horizontally averaged description of the canopy in the plot-scale surface-flux and radiation-exchange modules leads to further specific challenges in mixed canopies that are composed of trees belonging to more than one species, or trees of the same species that belong to different size

classes, and therefore have different hydrodynamics. Imagine a mixed canopy, checkerboard pattern of canopy-dominant trees: 50% of trees of species A and 50% of species B, with an LAI_p of 4. Assume species A and species B trees have the same crown-level leaf area index $LAI_c^{(sp)}$ (i.e., $LAI_c^{(A)} = LAI_c^{(B)} = 4$ [m^2 leaves of (sp) / m^2 ground under (sp) crowns]). The plot-scale, species-specific leaf area index $LAI_p^{(sp)}$ of both species A and B is 2 [m^2 leaves of (sp) / (m^2 ground)]. Imagine that species A trees are taller [10 m] than species B [8 m] and species A have thicker stems [DBH_A=20 cm] than species B [DBH_B=10 cm]. This hypothetical setup is illustrated in Figure 2 (top panel).

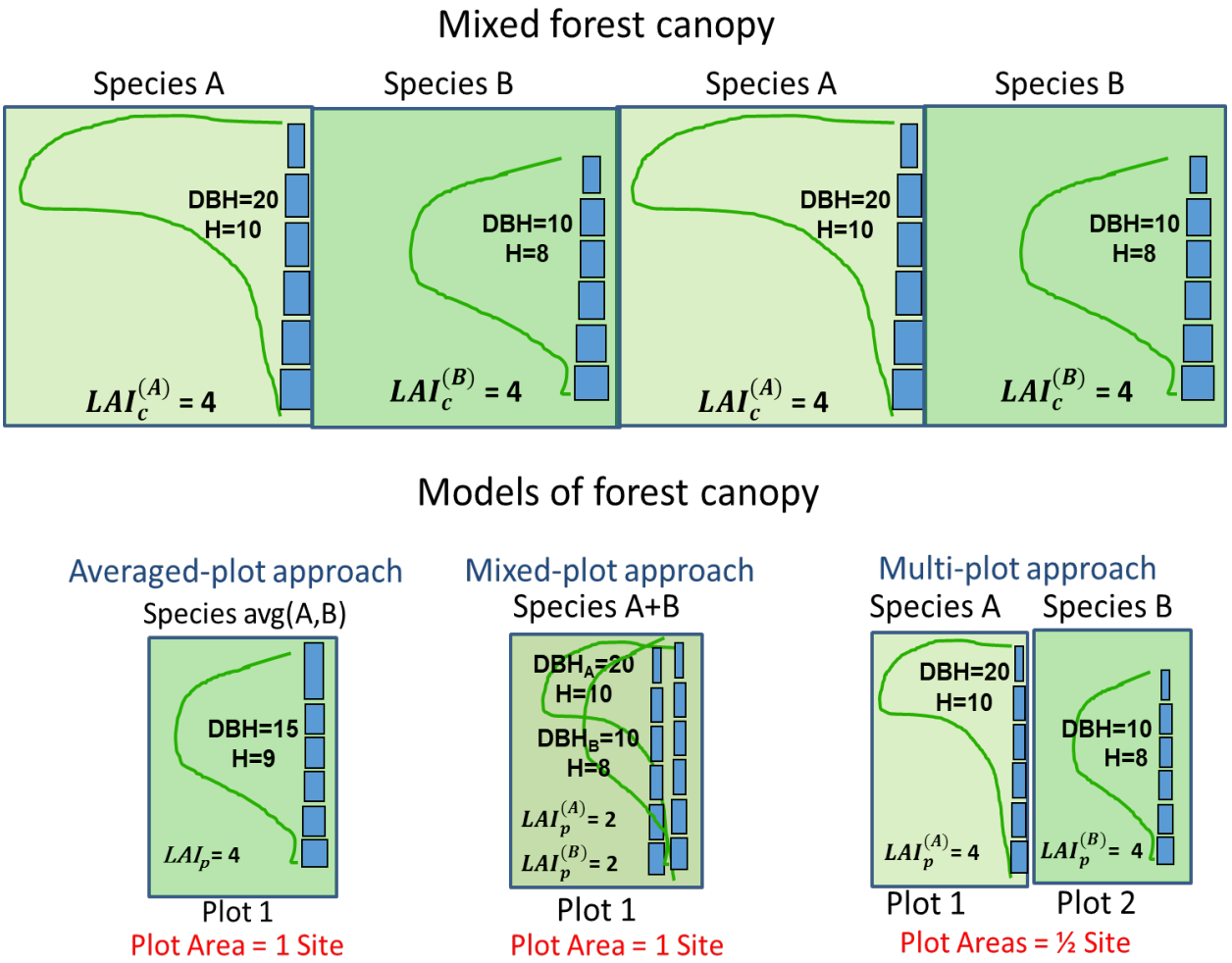

Figure 2. The "checkerboard-forest" conundrum – how to represent the canopy and crowns characteristics of a mixed forest site composed of two species of trees with different crown characteristics and hydraulic traits (top panel), in crown-level hydraulic models that need to represent the combination of crowns that make up the entire site? Three approaches, namely the averaged-plot approach, mixed-plot approach, and multi-plot approach, which are currently utilized in models, are represented in the bottom panels.

How could such a mixed forest (Fig. 2, top panel) be represented in hydrodynamic model? Current models take one of three approaches to solve this: (1) The averaged-plot approach resolves a single plot with a single characteristic tree type that represents the average of the two species in the original canopy (Fig. 2, bottom left). CLM-ml [*Bonan et al.*, 2018], CLM5 [*Song et al.*, 2020], and ELMv0 [*Liang et al.*, 2019] are examples of this approach. (2) The mixed-plot approach resolves two tree species co-filling the same plot, each with the assumed plot-scale properties of the tree species (Fig. 2, bottom center). ED2 [*Xu et al.*, 2016] and CLM-FATES [*Koven et al.*, 2020] are examples of this approach. (3) The multi-plot approach resolves a separate sub-site plot for each species, such that each plot is filled with a canopy composed of trees of only one species. Each sub-site plot occupies half of the area of the site (Fig. 2, bottom right). Most land surface models allow a multi-plot setup (as in approach 3) to represent different PFTs. As an example of this approach, *Cai et al.* [2019] demonstrates a multi-plot application of ELMv1 (the same model which Liang et al. 2019, referenced above, used in a single plot setup). Each of these approaches result in some bias due to the assumptions of scaling from tree to site scale. In the averaged-plot approach (1), the characteristics of the hydrodynamic model tree are not realistic and match none of the two species. In the mixed-plot approach (2), assuming that the number of stems is determined by a plot-level stand density, the stems of each of the tree species support half the leaf area that their crowns support in reality. The two species compete for light, which in the example above results in the taller species A always shading species B. In some cases, especially involving forest stands of mixed ages where the different species represent different age/size categories, this is a realistic description of the relationship between the two species. However, in a forest where the dominant canopy trees are of mixed species and grow side by side, both species are exposed to full sunlight, especially around noontime, despite species B being shorter on average. The multi-plot approach (3) results in hydrodynamically realistic trees; however, the environmental drivers of evaporative demand that each species experiences (e.g., temperature, humidity, and aerodynamic conductance) are calculated based on canopy characteristics particular to a single species rather than a realistic mixed canopy. The multi-plot approach is realistic when a forest is composed of large clusters of similar types/sizes of trees, as is often the case in silvicultural and heavily managed forests but is not a realistic representation of a mixed-canopy forest. In reality, scalar profiles, aerodynamic resistance, and the resulting wind profile inside a mixed canopy are horizontally mixed at spatial scales smaller than the turbulence eddy correlation length scale, and thus are characteristic of the mixed canopy, not a “pure” canopy of species-A or species-B crowns. In addition, the multi-plot approach also does not provide a realistic representation of water movement and water availability in the soil since these are influenced by the combined root characteristics of the different species in a mixed-canopy forest.

We propose a fourth approach that combines the advantages of the three approaches above. We will present a formulation that scales vegetation characteristics and the resulting fluxes from trees to forests in an energy and mass-conservative way and allows for a smooth and consistent multi-species canopy description for hydrodynamic models in mixed-forests.

2 Materials and Methods

2.1 Formulation - Canopy construction

We present the formulation for scaling hydrodynamic simulations of N_{sp} species of trees in a mixed forest. For simplicity, we refer to the categories of trees representing distinct hydraulic traits in the model as "species", but these could also represent different PFTs and/or different size categories within a PFT. These N_{sp} species co-occupy a single plot in a mixed canopy with assumed no (or low degree of) clustering among trees of the same species. In the model representation, characteristic tree-crown level dimensions will be used to specify N_{sp} individual virtual trees, each representing one species (sp). Each of these individual virtual crowns is resolved with multiple vertical layers, and for numerical simplicity, we assume that an identical vertical discretization of space is used for all species of trees in the canopy.

Within the model plot, the plant area density in the virtual tree crowns, a_{cz} [m^2 plant area / m^3 unit volume inside the crown], is composed of two components: the leaves, l_{cz}, and the stem area density, b_{cz} (i.e., $a_{cz} = l_{cz} + b_{cz}$). Plant area density can be measured directly with 3-D detail from airborne, spaceborne, or ground-based lidar. To represent the full crowns of multiple species co-occupying the same plot, a_{cz} values are organized in an array, $\mathbf{a_{cz}}$, with one column per species. Each column, $\mathrm{a}_{cz}^{(sp)}$, represents one model characteristic tree, and each row of the full matrix $\mathbf{a_{cz}}$ represents one vertical layer, z, throughout the vertical dimension of the canopy:

$$a_{cz_i}^{(sp)} \in \mathrm{a}_{cz}^{(sp)} = \begin{bmatrix} a_{z_{Nz}} \\ \vdots \\ a_0 \end{bmatrix}^{(sp)} \in \mathbf{a}_{cz} = \begin{bmatrix} a_{cz_{Nz}}^{(1)} & \dots & a_{cz_{Nz}}^{(N_{sp})} \\ \vdots & \ddots & \vdots \\ a_{c0}^{(1)} & \dots & a_{c0}^{(N_{sp})} \end{bmatrix} \quad (3)$$

such that the full array of plant area densities $\mathbf{a}_{cz}$ is composed of N_{sp} species-specific column vectors describing the vertical profiles of plant area density of each species, $a_{cz}^{(sp)}$, which are discretized to elements, $a_{cz_i}^{(sp)}$, in [m^2 leaf /m^3], describing the plant area density at the height above ground, z_i, of each vertical layer within the canopy for each crown type. The vertical discretization of the canopy is conducted such that the vertical spacing of each grid layer is constant, i.e., $z_{i+1} - z_i = \Delta z$. It is also uniform across all crown types; i.e., the number of vertical layers, N_z is such that the maximal height of the top vertical layer is at the height of the tallest crown type, i.e., $z_{Nz} = max\{h^{(1)}: h^{(Nsp)}\}$, where $h^{(sp)}$ is the crown-top height (commonly referred to as "canopy height") of each species, *sp*.

It is common to ignore the stem area density by assuming: $b_{cz} = 0$, at which point the plant area density profiles become identical to the leaf area density, $a_{cz} = l_{cz}$. For the purposes of calculating drag and light attenuation, ignoring stem/branch density is appropriate. However, b_{cz} is required for applications that use a plant hydrodynamic approach. Plant hydrodynamic models resolve the water movement and water potential through the xylem and thus require the conductive cross-section area of the xylem throughout the tree system. The species-specific active xylem conductive cross-section area, $\mathbf{bx}_{cz}^{(sp)}$ [m^2] is typically calculated using species-specific allometric equations of $\mathbf{b}_{cz}$ [*Matheny et al.*, 2014], which, in turn, is usually calculated using an allometric equation of $DBH^{(sp)}$, $A_c^{(sp)}$, and z. For deciduous species, $\mathbf{b}_{cz}$ can be directly observed by lidar measurements in the dormant season.

In mixed forests, lidar can be used to observe the plot-level leaf area density profile $\mathbf{l}_{pz}$ but, because it is impossible to distinguish species within a lidar point cloud, it cannot be used to directly observe $\mathbf{l}_{cz}^{(sp)}$. Ground-based lidar observations conducted under individual crowns are sometimes available, but typically an assumption must be made about the typical crown shape of each species. This assumption will be represented as a unit-normalized vertical profile of leaf density (i.e., when integrated vertically will sum to 1) and can be de-normalized to represent any tree of that type by multiplying the z axis of the normalized profile by $h^{(sp)}$ and multiplying the x axis by $LAI_c^{(sp)}/h^{(sp)}$. Note that by definition,

$$LAI_c^{(sp)} = \int_0^{z_{Nz}} l_{cz}^{(sp)} dz \simeq \Delta z \sum_{i=0}^{Nz} l_{cz_i}^{(sp)} \tag{4}$$

This approach can be used to combine plot-level observations of $LAI_c^{(sp)}$ and assumed allometric shapes of the crowns for each *sp* into a complete $\mathbf{l}_{cz}$ array, which is also consistent across scales from the resolved vertical layer to the whole crown. Furthermore, a plot-level leaf area density profile that represents the mean canopy characteristic leaf area per ground are over all tree types, $\mathbf{l}_{pz}$ (single column vector), can be formed from the normalized crown-level array, $\mathbf{l}_{cz,norm}$, and crown characteristics as:

$$\mathbf{l}_{pz} = \mathbf{l}_{cz}, norm \times \begin{bmatrix} \left(LAI_c^{(1)} \times A_c^{(1)} \times 0.0001 SD^{(1)}\right) \\ \vdots \\ \left(LAI_c^{(Nsp)} \times A_c^{(Nsp)} \times 0.0001 SD^{(Nsp)}\right) \end{bmatrix} \tag{5}$$

Where $\mathbf{l}_{cz,norm}$ provided the vertical distribution of leaf area from the ground to the crown top and integrates to 1.

A similar scaling approach is to be used independently to derive the plot-level, whole canopy $\mathbf{b}_{pz}$ (if needed and not assumed = 0) and then $\mathbf{a}_{pz} = \mathbf{l}_{pz} + \mathbf{b}_{pz}$. It is expected that $\mathbf{a}_{pz}$ and $\mathbf{l}_{pz}$ formed in this bottom-up approach by combining and scaling the individual species-specific profiles may diverge to some degree from directly observed full plot-level mean vertical profiles of leaf area distribution. This is because the sources of error associated with the species-specific estimates of plant and leaf area densities are different than those in the direct plot-level lidar measurements. Upon implementation, modelers should consider whether species-specific crown-level or whole-plot-level data are more important to preserve or could make slight modifications to each to optimize overall convergence with all scales of observations.

2.2 Multi-scale application – flux drivers

The purpose of any hydrodynamic module within a land surface model is to predict the sensible heat, latent heat, and carbon fluxes of the land surface, incorporating the effects of tree hydrodynamics on stomatal conductance. As such, any hydrodynamic module resolves a coupled set of functions for each surface flux. Each of the functions for surface fluxes requires multiple variables as drivers. These variables, specifically, the vertical profiles of net radiation, R_{nz}, air temperature, T_{cz}, humidity, q_{cz}, and wind speed U_{cz}, provide the values of the canopy environment that dictate the evaporative demand. Most models include a virtual entity for canopy air, embedded as a sub-grid-scale value (or set of values) within the lowest resolved atmospheric grid cell. The conditions in the canopy air are diagnosed (or prognosed, in models that resolve a fully coupled numerical scheme that link the surface fluxes and canopy air

conditions) as a function of the canopy characteristics (leaf density, roughness length) and the conditions in the open air above the canopy. Canopy air may be represented by a single bulk set of conditions or be vertically detailed.

Here, we discuss hydrodynamic models which resolve multiple species-specific, vertically resolved crowns, representative of a mixed canopy. Each of the species-specific crowns include a canopy air column with potentially different conditions. All the vertical canopy columns interact with a single, common, site-level atmospheric column. However, it is not obvious which canopy characteristics and at what scale best capture the relationship between the conditions in the open air above the canopy and the values of the vertical profiles of the flux drivers in the canopy air. For example, when resolving the specific-specific, crown-level R_{nz} at midday in the checkerboard mixed forest (Figure 2), the multi-plot approach which represents separate species-specific canopies will provide more realistic light attenuation profiles for each species than the mixed-plot approach, which will result in excessive shading over all trees of species B. However, wind speed, temperature, and humidity profiles are mixed inside the canopy at a length scale that is related to the eddy correlation scale and is typically larger than the size of individual tree crowns. Therefore, for T_{az}, humidity, q_{cz}, and wind speed U_{cz}, the mixed-plot and averaged-plot approaches will provide more realistic profiles than the multi-plot approach.

We propose a mixed approach, where vertical profiles of flux drivers are derived from canopy representations of different scales. Specifically, radiation should be characterized at the species-specific crown scale, i.e., $\mathrm{R}_{nz}^{(sp)} = f\left(\mathrm{l}_{\mathrm{cz}}^{(\mathrm{sp})}\right)$. Some unresolved issues for radiative transfer formulation are the reflection and long-wave emissions from the surrounding trees, which in a mixed forest do not have to originate from crowns of the same species and shading from near-by crowns when the sun is far from zenith (e.g., early in the morning). There are many different approaches and degrees of complexity to model within-canopy radiation conditions [see review of models participating in the RAMI intercoparisson project, *Widlowski et al.*, 2015; *Widlowski et al.*, 2011]. Some models, such as ACTS [*Ni-Meister et al.*, 2010; *Yang et al.*, 2010], are particularly suitable for hydrodynamic applications as they utilize a crown-based clumped approach and apply a crown-to-canopy scaling that utilizes crown diameter and stand density.

Flux drivers that are controlled by atmospheric surface layer mixing at typical length scales larger than a single tree crown (e.g, temperature, humidity, wind speed, and turbulent mixing) are characterized by the mean, whole-site canopy, e.g., $\mathrm{T}_{cz}^{(sp)} = f\left(\mathrm{l}_{pz}\right)$. Wind speed and turbulence mixing profiles through a canopy of prescribed vegetation density can be determined using 1st or 2nd order closure approaches [*Massman*, 1997; *Massman and Weil*, 1999]. One approach to predict within-canopy temperature and humidity utilizes the vorticity-thickness length scale [*Harman and Finnigan*, 2007; 2008].

Scaling of fluxes from crowns to forests

Any hydrodynamic model must represent a discrete virtual individual tree crown. Consequently, fluxes from the leaves to the air, whether prescribed per leaf area or per ground area, must be scaled over the leaf area of the crown to represent the fluxes that are supported by an individual stem. To illustrate that, imagine a tree with a stem diameter of 30 cm supporting a crown with a diameter of 10 m, and a given transpiration rate per leaf area. Compare this tree to a tree with a stem of the same diameter and same $LAI_c^{(sp)}$, but growing in a sparser canopy, such that the crown area is 1.5 times larger than that of the first tree. As the crown area, and with it the

total leaf area that are supported by the stem are larger, the sap flux (water per unit active xylem area) should be 1.5x larger, assuming xylem conductivity did not change. To preserve the conservation of mass through transport from the stem to the leaves and the air, hydrodynamic models must explicitly represent the crown by resolving flux from the leaves per leaf area, $F_{leaf}^{(sp)}$ [kg m^{-2} leaf s^{-1}], and multiply by the total leaf area of the crown $\left(LAI_c^{(sp)} \times A_c^{(sp)}\right)$ to get the total flow from a single crown, $F_{tree}^{(sp)}$ [kg s^{-1}].

The same flow (with time lag due to changes of water storage in the crown) will be transported through the conductive area of a single stem and consumed from the soil by the corresponding root system of that single virtual tree. This tree-level flow can be represented as a flux per ground area under the crown, $F_c^{(sp)}$, where:

$$F_c^{(sp)} = \frac{F_{tree}^{(sp)}}{A_c^{(sp)}} = F_{leaf}^{(sp)} \times LAI_c^{(sp)}. \quad (6)$$

$F_c^{(sp)}$ will have the units of [x/s/m^2 projected ground area under the crown], where x corresponds to the units of the flux in question, i.e., Joules for energy fluxes, kg for mass fluxes, etc. This representation of transpiration in terms of $F_c^{(sp)}$ is convenient since $LAI_c^{(sp)}$ and $A_c^{(sp)}$ must already be known in order to calculate flux drivers that are specified at the crown scale (e.g., radiation). In its most general form, scaling from each species-specific flux to the whole-plot flux to the atmosphere per unit ground area, F_p, is done as:

$$F_p = \sum_{sp}\left(F_{tree}^{(sp)} \times 0.0001 SD^{(sp)}\right). \quad (7)$$

When representing the tree-level flow in terms of $F_c^{(sp)}$, equation 7 becomes:

$$F_p = \sum_{sp}\left(F_c^{(sp)} \times A_c^{(sp)} \times 0.0001 SD^{(sp)}\right). \quad (7a)$$

Alternatively, from equation 2, the total leaf area of the crown could also be represented as $LAI_p^{(sp)}/0.0001SD^{(sp)}$, and $F_{tree}^{(sp)}$ could be represented as:

$$F_{tree}^{(sp)} = F_{leaf}^{(sp)} \times \frac{LAI_p^{(sp)}}{0.0001 SD^{(sp)}}. \quad (8)$$

We note that although equation 8 does not require knowledge of $LAI_c^{(sp)}$ or $A_c^{(sp)}$, these characteristics must be known in order to calculate crown-scale flux drivers. Thus, using either equation 7a or equation 8 requires knowledge of the same canopy characteristics.

5 Conclusions

Canopy construction for hydrodynamic models requires species-specific and whole-plot characteristics of the crowns and canopy. These include crown-level species-specific characteristics of $\boldsymbol{LAI_c^{(sp)}}$, $\boldsymbol{A_c^{(sp)}}$, and $\boldsymbol{SD^{(Nsp)}}$ (scalars), as well as the vertical profiles $\mathbf{a}_{cz}^{(sp)}$, $\mathbf{b}_{cz}^{(sp)}$ and $\mathbf{l}_{cz}^{(sp)}$ (vectors), and the species-specific plot-level $\boldsymbol{LAI_p^{(sp)}}$. From these characteristics the whole plot $\boldsymbol{LAI_p}$, $\mathbf{a}_{pz}$, and $\mathbf{l}_{pz}$ can be calculated, though these may also be independently observed. These crown, species, and whole-canopy characteristics provide a consistent multi-scale description of the canopy and provide all the required canopy characteristics needed to resolve and scale canopy fluxes.

Acknowledgments

We thank the support of the Ameriflux management project through core site US-UMB.

References

Atkins, J. W., G. Bohrer, R. T. Fahey, B. S. Hardiman, T. H. Morin, A. E. L. Stovall, N. Zimmerman, and C. M. Gough (2018), Quantifying vegetation and canopy structural complexity from terrestrial LiDAR data using the FORESTR R package, *Methods in Ecology and Evolution*, *9*(10), 2057-2066, https://doi.org/10.1111/2041-210X.13061.

Bohrer, G., H. Mourad, T. A. Laursen, D. Drewry, R. Avissar, D. Poggi, R. Oren, and G. G. Katul (2005), Finite-element tree crown hydrodynamics model (FETCH) using porous media flow within branching elements - a new representation of tree hydrodynamics, *Water Resources Research*, *41*(11), W11404, https://doi.org/10.1029/2005WR004181.

Bonan, G. B., E. G. Patton, J. J. Finnigan, D. D. Baldocchi, and I. N. Harman (2021), Moving beyond the incorrect but useful paradigm: reevaluating big-leaf and multilayer plant canopies to model biosphere-atmosphere fluxes – a review, *Agricultural and Forest Meteorology*, *306*, 108435, https://doi.org/10.1016/j.agrformet.2021.108435.

Bonan, G. B., E. G. Patton, I. N. Harman, K. W. Oleson, J. J. Finnigan, Y. Lu, and E. A. Burakowski (2018), Modeling canopy-induced turbulence in the Earth system: a unified parameterization of turbulent exchange within plant canopies and the roughness sublayer (CLM-ml v0), *Geoscientific Model Development*, *11*(4), 1467-1496, https://doi.org/10.5194/gmd-11-1467-2018.

Cai, X., W. J. Riley, Q. Zhu, J. Tang, Z. Zeng, G. Bisht, and J. T. Randerson (2019), Improving representation of deforestation effects on evapotranspiration in the E3SM land model, *Journal of Advances in Modeling Earth Systems*, *11*(8), 2412-2427, 10.1029/2018ms001551.

Christoffersen, B. O., et al. (2016), Linking hydraulic traits to tropical forest function in a size-structured and trait-driven model (TFS v.1-Hydro), *Geoscientific Model Development*, *9*(11), 4227-4255, https://doi.org/10.5194/gmd-9-4227-2016.

Dai, Y., R. E. Dickinson, and Y.-P. Wang (2004), A two-big-leaf model for canopy temperature, photosynthesis, and stomatal conductance, *Journal of Climate*, *17*(12), 2281-2299, https://doi.org/10.1175/1520-0442(2004)017<2281:atmfct>2.0.co;2.

Detto, M., H. C. Muller-Landau, J. Mascaro, and G. P. Asner (2013), Hydrological networks and associated topographic variation as templates for the spatial organization of tropical forest vegetation, *PLoS One*, *8*(10), e76296, https://doi.org/10.1371/journal.pone.0076296.

Farquhar, G. D., D. A. Walker, and C. B. Osmond (1989), Models of integrated photosynthesis of cells and leaves, *Philosophical Transactions of the Royal Society of London. B, Biological Sciences*, *323*(1216), 357-367, https://doi.org/10.1098/rstb.1989.0016.

Fisher, R. A., et al. (2018), Vegetation demographics in Earth System Models: A review of progress and priorities, *Global Change Biology*, *24*(1), 35-54, https://doi.org/10.1111/gcb.13910.

Garrity, S. R., K. Meyer, K. D. Maurer, B. S. Hardiman, and G. Bohrer (2012), Estimating plot-level tree structure in a deciduous forest by combining allometric equations, spatial wavelet analysis and airborne lidar, *Remote Sensing Letters*, *3*(5), 443–451, https://doi.org/10.1080/01431161.2011.618814.

Harman, I. N., and J. J. Finnigan (2007), A simple unified theory for flow in the canopy and roughness sublayer, *Boundary-Layer Meteorology*, *123*(2), 339-363, 10.1007/s10546-006-9145-6.

Harman, I. N., and J. J. Finnigan (2008), Scalar concentration profiles in the canopy and roughness sublayer, *Boundary-Layer Meteorology*, *129*(3), 323-351, 10.1007/s10546-008-9328-4.

Ju, Y., and G. Bohrer (2022), Classification of wetland begetation based on NDVI time series from the HLS dataset, *Remote Sensing Letters*, *14*, 2107, https://doi.org/10.3390/rs14092107.

Kennedy, D., S. Swenson, K. W. Oleson, D. M. Lawrence, R. Fisher, A. C. L. d. Costa, and P. Gentine (2019), Implementing plant hydraulics in the Community Land Model, version 5, *Journal of Advances in Modeling Earth Systems*, *11*(2), 485-513, 10.1029/2018MS001500.

Koven, C. D., et al. (2020), Benchmarking and parameter sensitivity of physiological and vegetation dynamics using the Functionally Assembled Terrestrial Ecosystem Simulator (FATES) at Barro Colorado Island, Panama, *Biogeosciences*, *17*(11), 3017-3044, https://doi.org/10.5194/bg-17-3017-2020.

Lawrence, D. M., et al. (2019), The Community Land Model Version 5: Description of new features, benchmarking, and impact of forcing uncertainty, *Journal of Advances in Modeling Earth Systems*, *11*(12), 4245-4287, https://doi.org/10.1029/2018MS001583.

Lefsky, M. A., W. B. Cohen, G. G. Parker, and D. J. Harding (2002), Lidar remote sensing for ecosystem studies, *Bioscience*, *52*(1), 19-30, https://doi.org/10.1641/0006-3568(2002)052[0019:LRSFES]2.0.CO;2.

Li, L., Z.-L. Yang, A. M. Matheny, H. Zheng, S. C. Swenson, D. M. Lawrence, M. Barlage, B. Yan, N. G. McDowell, and L. R. Leung (2021), Representation of plant hydraulics in the Noah-MP land surface model: model development and multiscale evaluation, *Journal of Advances in Modeling Earth Systems*, *13*(4), e2020MS002214, https://doi.org/10.1029/2020MS002214.

Liang, J., G. Wang, D. M. Ricciuto, L. Gu, P. J. Hanson, J. D. Wood, and M. A. Mayes (2019), Evaluating the E3SM land model version 0 (ELMv0) at a temperate forest site using flux and soil water measurements, *Geosci. Model Dev.*, *12*(4), 1601-1612, https://doi.org/10.5194/gmd-12-1601-2019.

Loveland, T. R., and A. S. Belward (1997), The IGBP-DIS global 1km land cover data set, DISCover: First results, *International Journal of Remote Sensing*, *18*(15), 3289-3295, https://doi.org/10.1080/014311697217099.

Massman, W. J. (1997), An analytical one-dimensional model of momentum transfer by vegetation of arbitrary structure, *Boundary-Layer Meteorology*, *83*(3), 407-421.

Massman, W. J., and J. C. Weil (1999), An analytical one-dimensional second-order closure model of turbulence statistics and the Lagrangian time scale within and above plant canopies of arbitrary structure, *Boundary-Layer Meteorology*, *91*(1), 81-107, 10.1023/A:1001810204560.

Matheny, A. M., G. Bohrer, C. S. Vogel, T. H. Morin, L. He, G. Mirfenderesgi, K. V. R. Schäfer, C. M. Gough, V. Y. Ivanov, and P. S. Curtis (2014), Species-specific transpiration responses

460 to intermediate disturbance in a northern hardwood forest, *Journal of Geophysical Research-*
461 *Biogeosciences*, *119*, 2292-2311, 10.1002/2014JG002804.
462 Ni-Meister, W., W. Yang, and N. Y. Kiang (2010), A clumped-foliage canopy radiative transfer
463 model for a global dynamic terrestrial ecosystem model. I: Theory, *Agricultural and Forest*
464 *Meteorology*, *150*(7), 881-894, https://doi.org/10.1016/j.agrformet.2010.02.009.
465 Schweiger, A. K., J. Cavender-Bares, P. A. Townsend, S. E. Hobbie, M. D. Madritch, R. Wang,
466 D. Tilman, and J. A. Gamon (2018), Plant spectral diversity integrates functional and
467 phylogenetic components of biodiversity and predicts ecosystem function, *Nature Ecology &*
468 *Evolution*, *2*(6), 976-982, https://doi.org/10.1038/s41559-018-0551-1.
469 Sellers, P. J., J. A. Berry, G. J. Collatz, C. B. Field, and F. G. Hall (1992), Canopy reflectance,
470 photosynthesis, and transpiration. III. A reanalysis using improved leaf models and a new
471 canopy integration scheme, *Remote Sensing of Environment*, *42*(3), 187-216,
472 https://doi.org/10.1016/0034-4257(92)90102-P.
473 Serbin, S. P., A. Singh, B. E. McNeil, C. C. Kingdon, and P. A. Townsend (2014), Spectroscopic
474 determination of leaf morphological and biochemical traits for northern temperate and boreal
475 tree species, *Ecological Applications*, *24*(7), 1651-1669, https://doi.org/10.1890/13-2110.1.
476 Simard, M., N. Pinto, J. B. Fisher, and A. Baccini (2011), Mapping forest canopy height globally
477 with spaceborne lidar, *Journal of Geophysical Research: Biogeosciences*, *116*(G4), G04021,
478 https://doi.org/10.1029/2011JG001708.
479 Song, J., G. R. Miller, A. T. Cahill, L. M. T. Aparecido, and G. W. Moore (2020), Modeling land
480 surface processes over a mountainous rainforest in Costa Rica using CLM4.5 and CLM5,
481 *Geoscientific Model Development*, *13*(11), 5147-5173, https://doi.org/10.5194/gmd-13-5147-
482 2020.
483 Sothe, C., M. Dalponte, C. M. d. Almeida, M. B. Schimalski, C. L. Lima, V. Liesenberg, G. T.
484 Miyoshi, and A. M. G. Tommaselli (2019), Tree species classification in a highly diverse
485 subtropical forest integrating UAV-based photogrammetric point cloud and hyperspectral
486 data, *Remote Sensing*, *11*(11), 1338, https://doi.org/10.3390/rs11111338.
487 Widlowski, J., et al. (2015), The fourth phase of the radiative transfer model intercomparison
488 (RAMI) exercise: Actual canopy scenarios and conformity testing, *Remote Sensing of*
489 *Environment*, *169*, 418-437, https://doi.org/10.1016/j.rse.2015.08.016.
490 Widlowski, J., et al. (2011), RAMI4PILPS: An intercomparison of formulations for the
491 partitioning of solar radiation in land surface models, *Journal of Geophysical Research:*
492 *Biogeosciences*, *116*(G2), G02019, https://doi.org/10.1029/2010JG001511.
493 Xu, X., D. Medvigy, J. S. Powers, J. M. Becknell, and K. Guan (2016), Diversity in plant
494 hydraulic traits explains seasonal and inter-annual variations of vegetation dynamics in
495 seasonally dry tropical forests, *New Phytologist*, *212*(1), 80-95,
496 https://doi.org/10.1111/nph.14009.
497 Yang, W., W. Ni-Meister, N. Y. Kiang, P. R. Moorcroft, A. H. Strahler, and A. Oliphant (2010),
498 A clumped-foliage canopy radiative transfer model for a Global Dynamic Terrestrial
499 Ecosystem Model II: Comparison to measurements, *Agricultural and Forest Meteorology*,
500 *150*(7), 895-907, https://doi.org/10.1016/j.agrformet.2010.02.008.
501 Yu, X., J. Hyyppä, P. Litkey, H. Kaartinen, M. Vastaranta, and M. Holopainen (2017), Single-
502 sensor solution to tree species classification using multispectral airborne laser scanning,
503 *Remote Sensing*, *9*(2), 108, https://doi.org/10.3390/rs9020108.
504